Biogenesis and Optimisation of Silver Nanoparticles by the Endophytic Fungus *Cladosporium sphaerospermum*

Sobhy I. I. Abdel-Hafez[1], Nivien A. Nafady[1], Ismail R. Abdel-Rahim[1], Abeer M. Shaltout[2] and Mohamed A. Mohamed[1,2,3].*

[1]Botany and Microbiology Department, Faculty of Science, Assiut University, Assiut 71516, Egypt.
[2]Plant Pathology Research Institute, Agricultural Research Center, Giza 12655, Egypt.
[3]Instituto de Biología Molecular y Celular de Plantas (Consejo Superior de Investigaciones Científicas - Universidad Politécnica de Valencia), Avenida de los Naranjos, 46022 Valencia, Spain.

Abstract: The present study is dealing with an ecofriendly and green biological route for extracellular biosynthesis of silver nanoparticles (AgNPs) using the endophytic fungus *Cladosporium sphaerospermum* F16 (KU199685). The biosynthesised AgNPs were characterised using ultraviolet-visible spectroscopy (UV-vis), transmission electron microscopy (TEM), dynamic light scattering (DLS), energy-dispersive X-ray analysis (EDX) and X-ray diffraction (XRD). The results showed the formation of stable, well-dispersed and spherical crystalline AgNPs with an average size 15.1 ± 1.0 nm and zeta potential of about -41.2 ± 0.5 mV. Optimisation of AgNPs synthesis prepared under different reaction conditions such as: pH, temperature, silver nitrate concentration and time of synthesis reaction to increase the AgNPs production. Meanwhile, the optimum conditions for maximum AgNPs production were pH (7), silver nitrate (5 mM) and incubation time (5-7 days). Interestingly, the fungal exo-metabolities were found to reduce silver ions into AgNPs within10 min after heating the reaction mixture (50-70 °C) as indicated by the developed reddish brown color compared to 30 min under room temperature.

Keywords: Silver nanoparticles, biosynthesis, optimisation, *Cladosporium sphaerospermum*.

1 Introduction

Nanotechnology is a fast-developing cutting-edge technology with wide-ranging applications in different areas of science and technology [1–4]. Metallic nanoparticles (MNPs) are considered the building blocks of the nanotechnology science and its broad applications [5-7]. Over the past decades, silver nanoparticles (AgNPs) over an attractive considerable interest among the emerging nanomaterials [8-11]. This may be backed to the fact of their excellent and unique electromagnetic, optical, catalytic properties, and their antimicrobial effects against numerous microbes including fungi, bacteria and viruses along with anti-proliferative effects compared with other metal nanoparticles [12-14]. On the other hand, their multi-applications as antiseptic, antimicrobial, anti-inflammatory, and their cytotoxic activity beside their used in dentistry, clothing, catalysis, mirrors, optics, photography, electronics and in the food packaging industry has tremendously increased its market value [15].

The synthetic route for the preparation of nanostructure materials and choosing the best optimised conditions to obtain well formed and maximum nanoparticles production are critically important in the current research, due to their physical properties which can be tailored for a specific application by controlling their size and morphology [16-17]. At present, there are many chemical and physical methods are involved in AgNPs synthesis, however those methods involve many hazardous chemicals as reducing agents such as hydrazine [18], sodium borohydride [19], and organic passivators such as thiophenol [20], thiourea [21], mercaptoacetate [22], etc., Which are toxic enough to pollute the environment if large scale nanoparticles are produced. Hence, there is a pressing need to develop clean, high yield, non-toxic, and environmentally benign synthesis processes for synthesis and assembly of nanoparticles [23].

Green chemistry approaches for the synthesis of AgNPs via biological methods using bacteria, fungi, plant extracts or purified bioactive compounds have helped to offer reliable and environmentally friendly alternatives to conventional chemical and physicals synthesis approaches [24-25]. Using microbes, especially their cell-free extracts, for the synthesis of AgNPs can be advantageous compared with

* Corresponding author E-mail: mohammed_sharouny@yahoo.com

other biological processes because microbial resources are abundant in nature, are easy to culture, and have the potential to be scaled up for large-scale synthesis [25-26]. Production of AgNPs through fungi has several advantages over other approaches. They include tolerance toward high metal nanoparticles concentration in the medium, easy management in large scale production of nanoparticles, good dispersion of nanoparticle and higher amounts of protein expression. As a result for large scale production of nanoparticles, fungi is preferred over other method.

Endophytic fungi are taxonomically and biologically diverse and dwell within robust plant tissue by having a symbiotic association. They have proven to be promising sources of new and biologically active natural products for exploitation in modern medicine, agriculture and industry [27].

Many important antifungal and antibacterial chemotherapeutics are either microbial metabolites or their semi-synthetic derivatives. *Cladosporium* constitutes one of the largest genera of hypomycetes, comprising more than 772 names [28] and commonly found as endophyte. *Cladosporium sphaerospermum* was isolated as endophytic fungus associated with various plant species [29-30]. In this study, a new approach to the highly efficient and rapid biosynthesis of metallic nanoparticles using the cell-free extract of the endophytic fungus *Cladosporium sphaerospermum* was investigated. Moreover, we studied the effects of some important reaction parameters including pH, temperature, silver nitrate concentration and time of incubation on AgNPs production to realize the best optimised conditions for maximum AgNPs production.

2 Material and Methods

2.1 Isolation of fungal endophytes

Four to six-months cultivated healthy tomato plants were collected from different localities in Qena Governorate, Egypt, June 2014. Monthly average temperatures are between 31 to 35 °C. Tomato plants were cultivated in these localities with commercial production systems with the use of pesticides and mineral fertilizers. Segments samples were taken from the middle portion of fresh healthy leaves and so all segments were surface sterilized with distilled H_2O, disinfected with 70% ethyl alcohol for one minute. The segments were directly transferred to 2.5% of sodium hypochlorite solution for 3.5 min, followed by 70% ethyl alcohol for 30 second. After washing with distilled H_2O, 5 segments of approximately 5x 5 mm placed on Petri dishes containing potato dextrose agar (PDA) medium supplemented with 250 mg L^{-1} streptomycin [31]. All inoculated plates were then incubated at 26 ± 2 °C for a period of 4 –7 days. The emergent mycelia were subcultured to new PDA plates for purification and finally incubated at 26 ± 2 °C for 7 days for identification.

2.2 Molecular identification of Cladosporium isolate

Among the isolated endophytic fungi, one isolate of *Cladosporium sphaerospermum* (isolated with relatively high frequency) was further chosen for molecular identification. For determination the ITS region of the rDNA fungal isolate, the frozen fungal mycelia (100 mg) were ground with liquid nitrogen in a mortar and pestle and mixed with 1 ml of 4 M guanidinium thiocyanate, 0.1 M sodium acetate pH 5.5, 10 mM ethylenediaminetetraacetic acid (EDTA), 0.1 M 2-mercaptoethanol. Extracts were clarified by centrifugation and supernatants were loaded into silica gel spin columns (Wizard Plus SV Minipreps DNA Purification, Promega, USA). Columns were washed with 70% ethanol, 10 mM sodium acetate pH 5.5, and DNA eluted with 50 µl of 20 mM Tris-HCl, pH 8.5.

2.2.1 Ribosomal DNA amplification and sequencing

The ribosomal internal transcribed spacer (ITS) region of the rDNA fungal isolate was amplified by PCR using primer pairs ITS1 (5'-CTTGGTCATTTAGAGGAAGTAA-3') and ITS4 (5'-TCCTCCGCTTATTGATATGC-3') [32]. PCR amplification was carried out for ITS1 and ITS4 in an i-cycler (Bio-Rad, Hercules, CA, USA) for 30 cycles of 94 °C for 1 min (denaturing), 55 °C for 1 min (annealing) and 72 °C for 150 s (extension). Initial denaturating at 94 C was extended to 5min and the final extension was for 10 min at 72 °C. PCR products were separated by electrophoresis in a 1% agarose gel run for 75 min in TAE buffer (40 mM Tris, 20 mM sodium acetate, 1 mM EDTA, pH 7.2) and viewed using a UV transilluminator after ethidium bromide staining. According to electrophoretic migration, the PCR products that corresponded to the ribosomal ITS were eluted from the gel using silica spin columns (DNA Clean & Concentrator, Zymo Research). The purified double strands PCR fragments were directly sequenced with BigDye terminator cycle sequencing kits (applied Bipsystems, foster city, CA, USA) by following the manufacturer's instructions. The consensus sequences were employed to search for homologous sequences with the BLAST search program at the National Center for Biotechnology Information (NCBI; http://www.ncbi.nlm.nih.gov).

2.3 Biogenesis of AgNPs

For biogensis of AgNPs, the fungal biomass of *Cladosporium sphaerospermum* isolate was grown aerobically in sterilised conical flasks containing potato dextrose (PD) medium. The inoculated flasks were agitated at 120 rpm on orbital shaker and incubated for 3 days at 26 ± 2 °C. After the incubation period, the grown fungal

biomass was extensively washed using deionised water to remove all medium component from the biomass.

In general, 10 g (wet weight) of the cleaned fungal biomass was brought in contact with 100 mL sterile deionised water in an Erlenmeyer flask and agitated at 120 rpm and incubated for 2 days at 26 ± 2 $^\circ$C. After 2 days, the cell filtrate was filtered through Whatman filter paper No. 1 and the filtrates were treated with 100 ml of 1 mM silver nitrate (AgNO$_3$, Sigma Aldrich) solution in an Erlenmeyer flask and incubated at room temperature in dark to avoid photoreduction. The cell-free filtrate without silver nitrate solution and silver nitrate solution were used as controls under similar experimental conditions and the color change was observed up to 48 h [33].

2.4 Characterisation of AgNPs

2.4.1 UV-Vis spectroscopic analysis

The formation and stability of AgNPs were preliminarily confirmed by visual observation of color change from pale white to pale brown and further confirmed followed by UV–vis spectrophotometry. A small aliquot (2 mL) of the suspended particles was taken in a quartz cuvette and observed for wavelength scanning ranging between 300-800 nm at different time intervals with distilled water as a blank solution. PerkinElmer Lambda 950 UV/Vis spectrometer was used for UV visible spectroscopy. Stability of bio reduced silver nanoparticles was analysed using UV–Vis absorption spectra. For this, 4-fold diluted solution was prepared. The colored mixture was then centrifuged at 15,000 rpm for 15 min and washed three times with de-ionized distilled water, and finally dried at 60°C.

2.4.2 High resolution transmission electron microscopy (HR-TEM)

The transmission electron microscopy was applied to measure the size and study the morphological characters of the biosynthesised AgNPs. For HR-TEM measurements, 3 µl of the sample solution was pipetted onto a carbon-coated copper grid (carbon type-B, 300 mesh, Ted Pella, Inc., Redding, CA, USA). The sample-loaded grid was air dried under vacuum desiccation for 3 h. The TEM micrograph images were obtained using JEOL instrument 1200 EX instrument on carbon coated copper grids operated at an accelerating suitable voltage (kV).

2.4.3 Dynamic light scattering (DLS)

The dynamic light scattering (DLS) analysis was used to measure the AgNPs size and their distribution in the solution. To estimate the particle size, a dilute suspension of AgNPs was prepared in deionized water and sonicated for removing aggregation at 35 °C for 20 min and then subjected to DLS analysis. The average particle size and zeta potential of nanoparticles were estimated using a Zetasizer, Nano-ZS90 system (Malvern Inc., Malvern, UK).

2.4.4 Energy Dispersive X-ray photometric analysis (EDX)

EDX analysis was also performed by energy-dispersive spectroscopy (EDS) using INCA Energy TEM 200 with analysis software (JEOL) for identifying the elemental composition of the biosynthesised AgNPs.

2.4.5 X-ray diffraction analysis (XRD)

Crystalline metallic pattern of silver nanoparticles powder was analysed using X-ray diffraction. In order to obtain a pellet of pure AgNPs for XRD analysis, reaction medium was centrifuged by 4-5 cycles at 18,000 rpm for 15 min followed by re-dispersion in deionized water. The X-ray diffraction (XRD) patterns were then conducted to X-ray diffraction analysis carried out using Phillips PW 1830 instrument Powder (Phillips, USA). The operating voltage of 40 kV and current of 30 mA with Cu kα radiation of 0.1541 nm wavelength, in the 2θ range 10-80° angle [34].

2.5 Optimisation of silver nanoparticles production

For large scale production and stable mycofabrication of AgNPs, different parameters including pH, temperature, concentration of silver nitrate (AgNO$_3$) and time of reaction was studied. The optimum conditions of reaction parameters were selected by measuring the absorbance of the resulting solutions spectrophotometrically. For each condition, respective controls were maintained.

2.5.1 Effect of different pH values

The influence of pH on synthesis and stability of AgNPs was studied under different pH values of the cell free fungal filtrate (pH 3, 5, 7 and 9) and the filtrate was maintained by 1 N HCl and 1 M NaOH.

2.5.2 Effect of temperatures

Effect of different temperatures on the rate of synthesis and production of AgNPs was studied in which the fungal filtrate after treating with 1 mM silver nitrate kept at different temperature ranging from 0°C, 15°C, 30°C, 50°C and 70°C.

2.5.3 Effect of Silver nitrate concentrations and time of incubation

The effect of different concentrations of silver nitrate (1, 3, 5 and 10 mM) on the synthesis of nanoparticles was evaluoated. Also, the stability of AgNPs through a time

course was studied by measuring UV–vis spectra after regular interval of 0 min, 1h, 5h, 24h,1 week and 1 month.

3 Results and Discussion

3.1 Identification of the endophytic fungi

Seventy-three fungal strains were initially recovered from 50 tomato leaf fragments collected from sites under study. Among those, 8 fungal species representing 5 genera were morphologically identified, while two did not form reproductive structures (sporophores and spores), which were termed morphotaxa 1 and 2 (Table 1). There were differences in endophyte species frequency and the most predominant genus was *Cladosporium* which showed 56% colonisation frequency. *Trichoderma* occupied the second grade and was recovered in moderate occurrence and frequency (12 and 24%, respectively). Among the species, *Cladosporium sphaerospermum* **Penzig** was the most prevalent and isolated in high frequency (36%) while *Aspergillus nidulans* **(Eidam) Winter** was the lowest in the frequency (4%).

Table 1: The number of records and the colonization frequency (%) of endophytic fungi isolated from healthy tomato leaves.

Endophytic fungi	No. of records	Frequency (%)
Aspergillus niger **Tiegh.**	5	10
Aspergillus terrus **Thom**	5	10
Cladosporium cladosporioides (Fresen.) G.A. de Vries	10	20
Cladosporium sphaerospermum **Penzig**	18	36
Emericella sp. **Berk.**	4	8
Fusarium oxysporum **Schlecht emend. Snyder & Hansen**	8	16
Penicillium chrysogenum **Westling**	9	18
Trichoderma harzianum **Rifai**	12	24
Morphotaxon 1	1	2
Morphotaxon 2	1	2

Colonies of the most abundant species *Cladosporium sphaerospermum* on PDA plates were 9.5-11 mm and 10.0-13.0 mm in diameter, respectively, after 7 days at 26 ± 2 °C. Colonies were olivaceous to grey-olivaceous on PDA, revere side of the colonies were greenish-black, with a margin that was either regular or radially furrowed, having a wrinkled colony centre and formed a crater-like structure (Fig. 1 A). Conidiophores are variable in length, up to 300 µm long and 3-5 µm wide, smooth-walled or verrucose and not nodose. Conidia were spherical, ellipsoidal to cylindrical with sounded ends, single celled, verrucose with dimensions of 2.0-8.0 X 2.0-4.0 µm (Fig.1 B) [35-36].

The most abundant fungal strain was used for further molecular identification using phylogenetic analysis of 18S rRNA gene sequences. As a result, a partial 18S rRNA gene sequences of approximately 1029 base pairs of fungal strain F16 has a sequence with 99% identity match with *Cladosporium sphaerospermum* (KC311475) in NCBI GenBank, so the isolated fungal strain identified as *Cladosporium sphaerospermum* (KU199685).
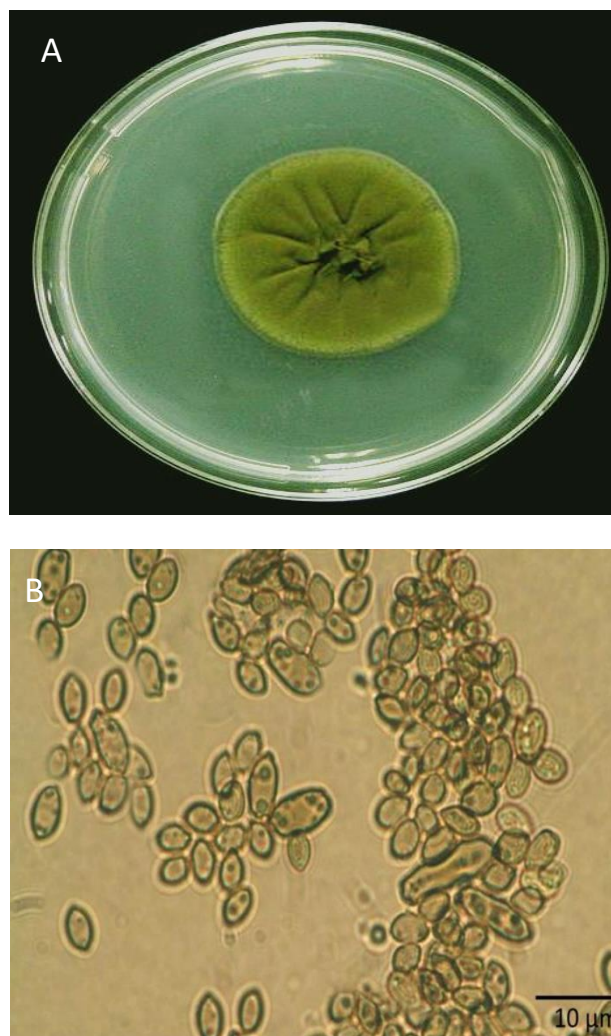

Fig.1: *Cladosporium sphaerospermum*. (A) 5 days old culture at 26 ± 2 °C on PDA medium; (B) Microscopic features showing the fungal conidia.

3.2 Biosynthesis of silver nanoparticles

The possibility of biosynthesis AgNPs using the cell-free supernatant of *Cladosporium sphaerospermum* F16 (KU199685) was studied. During the incubation period, the results showed changing the colour mixture of silver nitrate with the fungal extract to pale brown, which is a clear indication of the formation of silver nanoparticles [37]. Silver nanoparticles are known to exhibit unique optical

properties due to the surface plasmon resonance (SPR). The UV–Vis spectroscopic analysis of the biosynthesised AgNPs solution showed a strong absorbance peak centred at 435 nm which is characteristic for SPR of silver and hence indicates the formation of AgNPs (Fig.2 A). This color occurs due to excitation of surface plasmon vibrations in AgNPs [38]. Moreover, the increase in the absorbance of AgNPs was easily observed with a prolonged reaction time, which indicated a greater reduction of Ag^+ ions and the formation of more AgNPs. Control silver nitrate solution neither developed the brown color nor did they display the characteristic band (Fig.2 B).

3.3 Characterisation of AgNPs

The size and morphology of the biosynthesised AgNPs were examined by HR-TEM (Fig. 3). TEM and DLS measurements showed the formation of well dispersed and spherical AgNPs with an average size distribution of 15.1 ± 1.0 nm (Fig. 3, 4). A negative zeta potential of about −41.2 ± 0.5 mV was also observed during the presrnt work (Fig. 5). The high absolute value of zeta potential clearly revealed the presence of high electrical charge on the AgNPs surface, as a result strong repulsive force may be
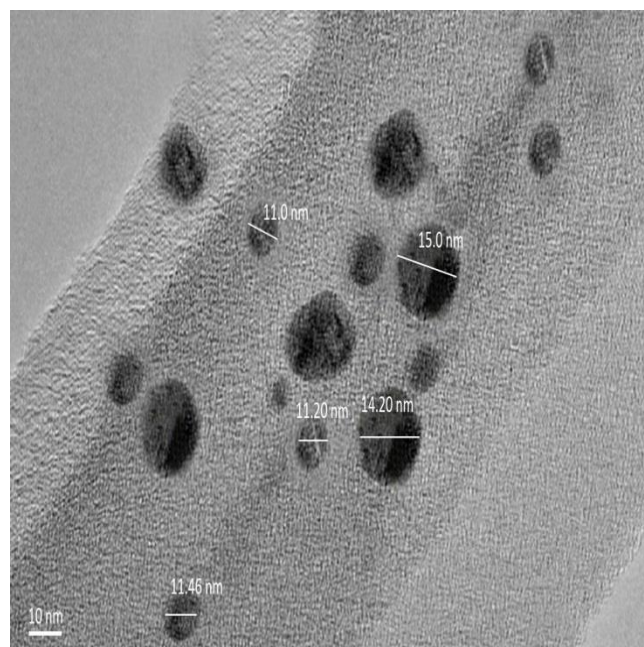

Fig.3. : High-resolution -TEM image of the biosynthesised AgNPs.

formed among the particles spaces which prevent agglomeration and indicate a very stable AgNPs in the colloidal state. EDX analysis gives qualitative as well as quantitative status of elements that may be involved in formation of nanoparticles. The elemental profile of synthesised nanoparticles using *C. sphaerospermum* fungal extract showed typical optical absorption peak at approximately 3 keV, which was attributed to the SPR of the metallic Ag nanocrystals and confirms the formation of silver nanoparticles [39] (Fig. 6).
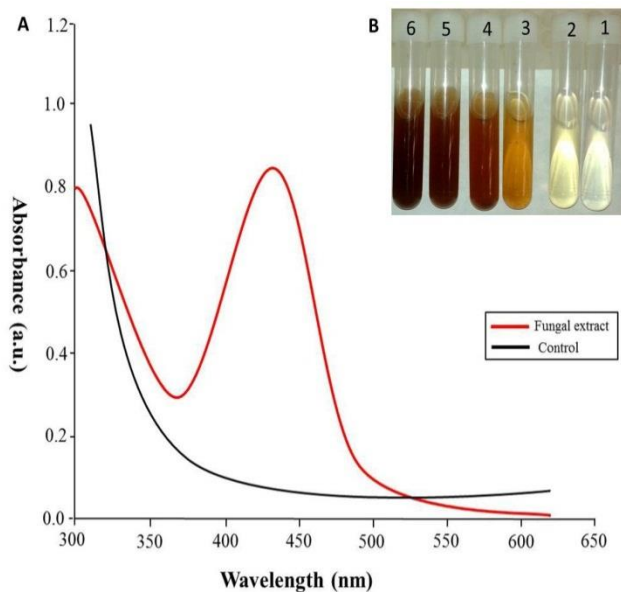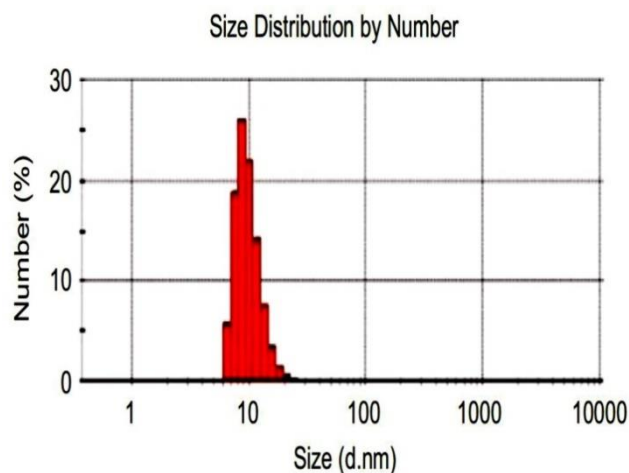

Fig.2: Biosynthesis of AgNPs using the cell free supernatant of *Cladosporium sphaerospermum*: (A) Surface plasmon spectra of the biosynthesized AgNPs; (B) Changing in color of silver nitrate solution after reduction of Ag+ ions and formation of AgNPs, (1= silver nitrate, 2= fungal extract, 3-6= Continued increase in the intensity of yellow brown colour with increase in time (contact time: 0, 1h, 5h and 24h).

Fig. 4: Dynamic light scattering measurements for particle size distribution of the biosynthesized AgNPs.
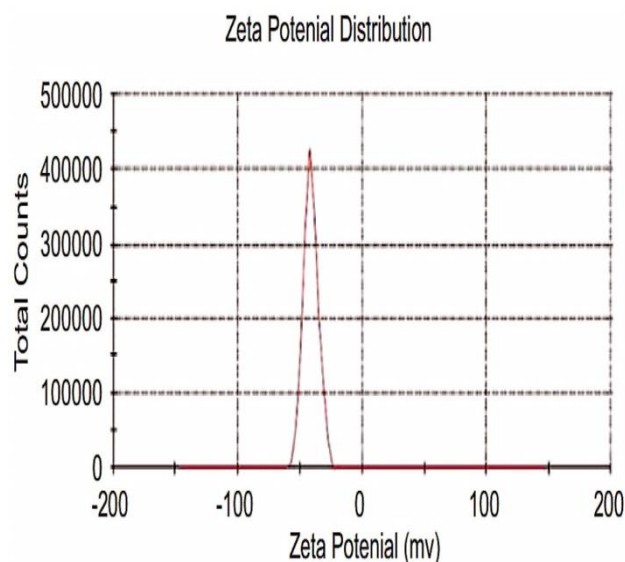
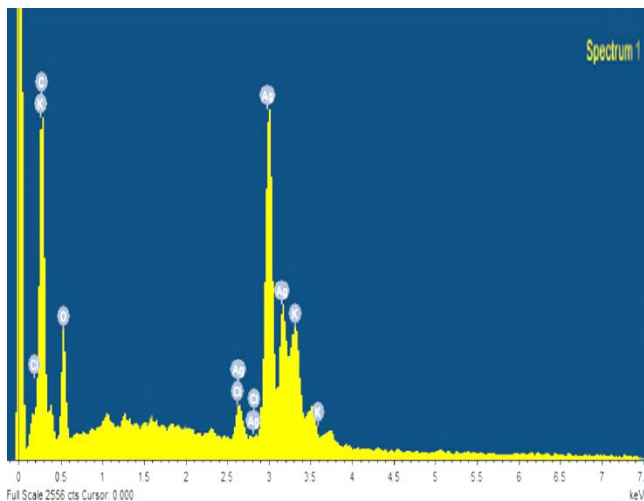**Fig. 5:** Zeta potential measurements of the biosynthesized AgNPs

Fig. 6: EDX spectrum of the biosynthesised AgNPs.

The formation of silver nanoparticles was further supported by XRD measurement (Fig. 7). The Bragg reflections corresponding to the (111), (200), (220), (311), and (222) sets of lattice planes were observed that might be indexed on the basis of face-centered cubic (fcc) structure of metallic silver (JCPDS file no. 00- 004-0783). The broad nature of the XRD peaks could be attributed to the nanocrystalline nature of the AgNPs.

3.4 Optimisation of AgNPs production

To increase the AgNPs synthesis rate, medium optimisation processes were carried out under different physicochemical conditions.
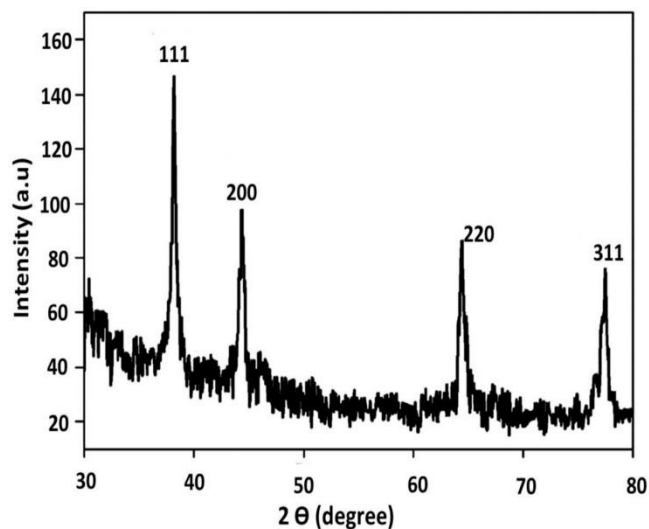

Fig. 7: X-ray diffraction patterns of the biosynthesised AgNPs.

3.4.1 Effect of pH

The color of reaction mixture and the intensity of the absorbance peaks were pH dependent. The UV–Vis spectra recorded from the reaction medium at different pH values showed that the maximum AgNPs production (0.73 a.u.) was at pH = 7 and with increase in pH till 9, a little bite increase was also recorded in the UV color intensity value (0.80 a.u.) (Fig. 8 A, B). On the other hand, in acidic conditions we cannot observe any characteristic absorbance band for AgNPs formation. These results revealed that, pH value started from 7 to 9 supported the maximum synthesis of AgNPs nanoparticles (Fig. 8 B) and this in agreement with those findings of Baghizadeh et al. [40].

Moreover, Roopan et al. [41] reported also that at pH 2.0 no reaction occurred while at pH (7-11) highly monodispersed nanoparticles were obtained. Different reports suggested that a variety of biomolecules are involved in biological nanoparticle synthesis, such biomolecules are likely to be inactivated like polysaccharides and proteins under the extremely acidic conditions (pH 3.0) and start to work effectively in neutral and slightly alkaline conditions [42-44]. On another hand, the noticeable difference in the mixture colors obtained over the range of pH could be ascribed to a variation in the dissociation constants (pKa) of functional groups on the biomass that are involved [45-47].
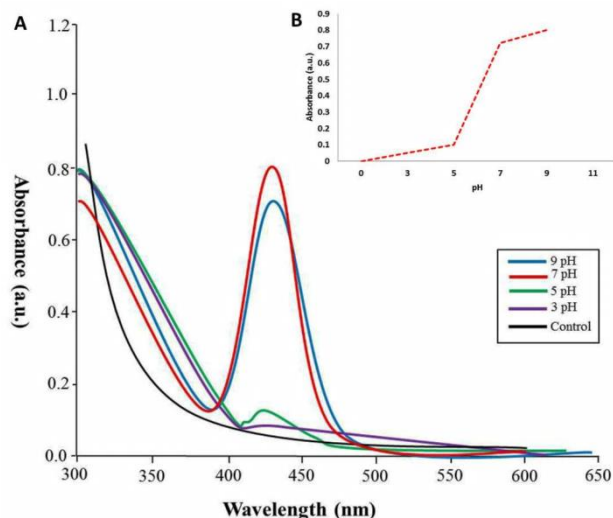
Fig. 8: (A) UV–vis spectrum of AgNPs at different pH values; (B) Effect of pH values on absorbance intensity of the biosynthesized AgNPs.

3.4.2 Effect of temperature

The temperature also plays an important role in acceleration the process of AgNPs production. During the present study, it was observed that the reaction mixtures incubated at 0, 15 °C beard light reddish brown color with less pronounced SPR peaks. In contrast, at higher incubation temperature (50 and 70 °C) dark reddish brown color and more intense absorbance peaks were revealed (Fig. 9).
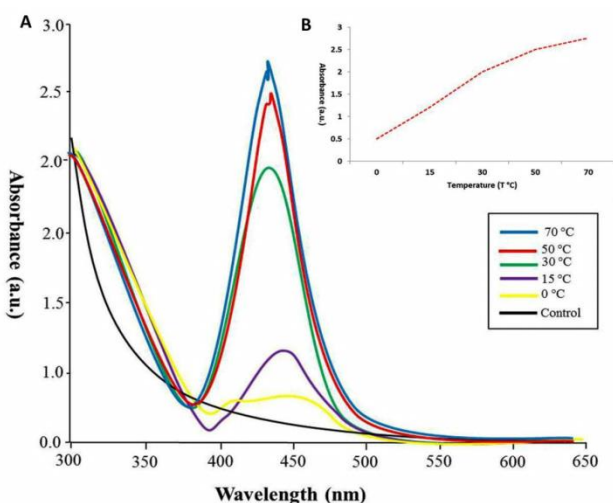

Fig. 9: (A) UV–vis spectrum of AgNPs at different reaction temperature; (B) Effect of reaction temperature on absorbance intensity of the biosynthesised AgNPs.

Interestingly, at room temperature (30 °C) the formation of AgNPs accompanied with the color change after 30 min. However, at 50 – 70 °C the Ag reduction process and formation of AgNPs was noticed faster and the reddish brown color was developed after only 10 min. The maximum SPR peak intensity was detected at 70 °C. The

results revealed also that by increasing in the reaction temperature, a sharp narrow UV spectra peak at lower wavelength region (412 nm at 70 °C) are developed, which indicate the formation of smaller nanoparticles, whereas, at lower reaction temperature, the peaks observed at higher wavelength regions (440 nm at 30 °C) which clearly indicates increase in silver nanoparticles size. Those findings are in agreement with the fact that when the temperature is increased, the reactants are consumed rapidly leading to the formation of smaller nanoparticles [48].

3.4.3 Effect of Silver nitrate concentration

Changing in substrate concentration clearly indicated that AgNPs formation increases with increase in $AgNO_3$ conc. up to 5 mM (Fig. 10 A, B). With further increase, no more noticeable increase in nanoparticle formation within 24 h. Interestingly, the reduction rate of the AgNPs ions with 5 mM concentration was nearly completed after 1 h compared with 7 days before concentration optimisation. This finding is quite interesting as it contradicts the report of Kathiresan *et al.* [49] who used *Penicillium fellutanum* fungal strain. They found decrease in optical density after 1 mM substrate concentration and accordingly they proposed 1mM substrate concentration as the optimal AgNPs production condition.
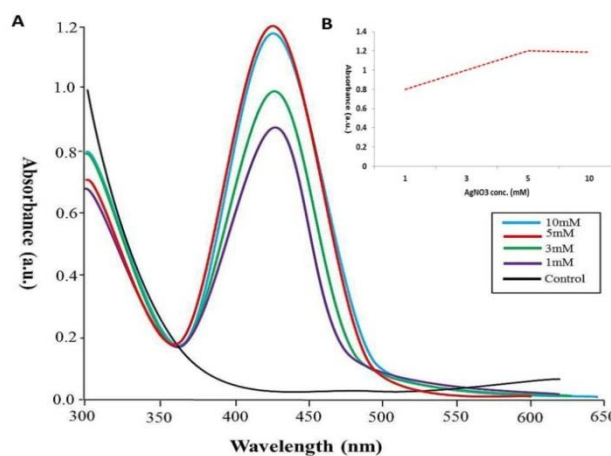

Fig. 10: (A) UV–vis spectrum of AgNPs at different concentrations of silver nitrate solution; (B) Effect of silver nitrate concentrations on absorbance intensity of the biosynthesised AgNPs.

3.4.4 Effect of incubation time

The rate of AgNPs absorbance intensity was directly proportional to the incubation time of its mixture. The obtained results clearly revealed that the rate of Ag+ ions reduction and formation of AgNPs was going slowly during the first hour of incubation, as indicated by the low color intensity (0.25 a.u.) at 435 nm wavelength value (Fig. 11). up to 168 h as shown in Fig. 11 (A, B). The maximum reduction of Ag+ ions was obtained after one week. The

increase in absorbance along with color intensity could be backed to an increase in the number of AgNPs formed with time [50-51]. It has been reported that the time required for complete reduction of the metal ions during biosynthesis process of metal nanoparticles using microbes range from 24 to 124 h [52]. The UV-vis absorption spectra clearly indicated high stability of the formed AgNPs after being stored for one month at room temperature (see Fig. 11).
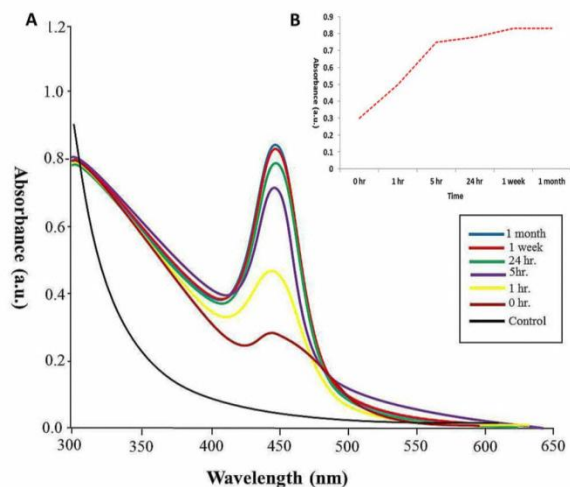

Fig. 11: (A) UV–vis spectrum of AgNPs at different reaction time; (B) Effect of reaction time on absorbance intensity of the biosynthesised AgNPs).

4 Conclusion

In this study, we have demonstrated a green synthesis of high purity AgNPs with the features of simplicity, high reduction rate, and high yield using aqueous extract of the endophytic fungal *Cladosporium sphaerospermum*. The fungal extract was used as both reducing and capping agent in the AgNPs formation. The formed AgNPs were highly stable, spherical in shape, well dispersed and crystalline in nature with an average size 15.1 ± 1.0 nm and zeta potential of about -41.2 ± 0.5 mV at optimum conditions. Moreover, it was indicated that the optimum conditions for maximum AgNPs production were pH (7), silver nitrate (5 mM) and incubation time (5-7 days).

Interestingly, the fungal extract were found to reduce silver ions into AgNPs within10 min after heating the reaction mixture (50-70 °C) as indicated by the developed reddish brown color and confirmed by UV visible spectra compared to 30 min under room temperature. Undoubtedly, this green synthesis approach appears to be a cost-effective, non-toxic, ecofriendly alternative method to the conventional microbiological, physical and chemical ones, and would be suitable for developing a biological process for large-scale production.

Acknowledgment

References

[1] H. Karimi-Maleh, P. Biparva, M. Hatami, *Biosensors and Bioelectronics*, 48, 270–275, (2013)

[2] R. Moradi, S.A. Sebt, H. Karimi-Maleh, R. Sadeghi, F. Karimi, A. Bahari, H. Arabi, *Physical Chemistry Chemical Physics*, 15, 5888–5897, (2013)

[3] R. Sadeghi, H. Karimi-Maleh,M.A. Khalilzadeh, H. Beitollahi, Z. Ranjbarha, M.B. Pasha Zanousi, *Environmental Science and Pollution Research*, 20(9), 6584-6593, (2013).

[4] M. Elyasi, M.A. Khalilzadeh, H. Karimi-Maleh, *Food Chemistry*, 141, 4311–431, (2013).

[5] R. Rotello, V.M. Shenhar, *Accounts of Chemical Research*, 36(7): 549–561, (2003).

[6] P.H. Davis, C.P. Morrisey, S.M.V. Tuley, C.I. Bingham, *American Chemical Society*, Washington DC, pp. 2–14, (2008).

[7] M. Rai, N. Duran, *Metal Nanoparticles in Microbiology*. Springer, New York, (2001).

[8] L.A. Austin, M.A. Mackey, E.C. Dreaden, M.A. El-Sayed, Archives *of toxicology*, 88(7), 1391-1417.

[9] W.P. McConnell, J.P. Novak, L.C. Brousseau, R.R. Fuierer, R.C. Tenent, D.L. Feldheim, *Journal of Physical Chemistry B*, 104(38), 8925-8930, (2000).

[10] A. Majdalawieh, M.C. Kanan, O. El-Kadri, S.M. Kanan, Journal of nanoscience and nanotechnology, 14(7), 4757-4780,(2014).

[11] T. Prathna, A.M. Raichur, N. Chandrasekaran, A. Mukherjee. *Reviews in Advanced Sciences and Engineering*, 3(3), 239-249, (2014).

[12]. M. Gajbhiye, J. Kesharwani, A. Ingle, A. Gade, M. Rai. *Nanomedicine: Nanotechnology, Biology and Medicine*, 5(4), 382-386, (2009).

[13] A. Panacek, L. Kvítek, R. Prucek, M. Kolar, R. Vecerova, N. Pizúrova, V.K. Sharma, T. Nevecna, R. Zboril. *Journal of Physical Chemistry B*, 110, 16248–16253, (2006).

[14] Y. Qian, H. Yu, D. He, H. Yang, W. Wang, X. Wan, L. Wang. *Bioprocess and biosystems engineering*, 36(11), 1613-1619, (2013).

[15] M. Ghaffari-Moghaddam, R. Hadi-Dabanlou, *Journal of Industrial and Engineering Chemistry,* 20(2), 739-744, (2014).

[16] N. Durán, P.D. Marcato. *Springer Berlin Heidelberg*, (2012).

[17] P.K. Sahoo, S.S.K. Kamal, T.J. Kumar, B. Sreedhar, A.K. Singh, S.K. Srivastava. *Defence Science Journal*, 59, 447–455, (2009).

[18] B.M. Choudary, S. Madhi, N.S. Chowdari, M.L. Kantam, B. Sreedhar. *Journal of the American Chemical Society*, 124: 14127–14136, (2002).

[19] Y. Wang, M.H. Du, J.K. Xu, P. Yang, Y.K. Du. *Journal of Dispersion Science and Technology* 29, 891–894, (2008).

[20] T.R. Ravindran, A.K. Arora, B. Balamurugan, B.R. Mehta. *Materials Research Innovations* 13(1) 32-34, (2009).

[21] M. Pattabi, J. Uchil, *Solar Energy Mater Solar Cell* 63:309–314 (2000) doi:10.1016/S0927-0248(00)00050-7.

[22] S.M. Liu, F.Q. Liu, H.Q. Guo, Z.H. Zhang, Z.G. *Solid State Communications*, 115(11), 615-618, (2000).

[23] S. Mohan, O.S. Oluwafemi, S.C. George, V.P. Jayachandran, F.B. Lewu, S.P. Songca, N. Kalarikkal, S. Thomas. *Carbohydrate Polym Journal*, 106 469–474, (2014)

[24] F.M. Morsy, N.A. Nafady, M.H. Abd-Alla, D.A. Elhady. *Universal Journal of Microbiology Research*, 2(2), 36-43, (2014).

[25] M.A. Mohamed. *International Journal of Nanomaterials and chemistry*, 1(3), 103 110, (2015).

[26] K.B. Narayanan, N. Sakthivel. *Advances in colloid and interface science*, 156(1), 1-13, (2010).

[27] G.A. Strobel. *Critical reviews in biotechnology*. 22(4), 315-333, (2002)

[28] F. M. Dugan, K. Schubert, U. Braun. *Schlechtendalia*, 11:1-103, (2004).

[29] N. C., Paul, S. H. Mycobiology, 36(4), 211-216, (2008).

[30] S. Hodgson, C. Cates, J. Hodgson, N. J. Morley, B. C. Sutton, A. C. Gange .*Ecology and evolution*, 4(8), 1199-1208, (2014).

[31] N.R. Smith, T.V. Dawson. *Soil science*, 58(6) 467-472, (1944).

[32] M. Gardes,T.D. Bruns. *Molecular ecology*, 2(2), 113-118, (1993).

[33] A.M., Fayaz, C.S. Tiwary, P.T.V. Kalaichelvan, R. P.T,Venkatesan. *Colloids Surf B Biointerfaces*; 75:175–8 (2010).

[34] B. Cullity, Elements of XRD. USA Edison-Wesley P Inc., 1978.

[35] H.C. Gugnani, V. Ramesh, N. Sood, J. Guarro, *Medical Mycology*, 44, 285e288, (2006).

[36] P. Zalar P, G.S.de Hoog, H.J. Schroers, P.W. Crous, J.Z. Groenewald. *Studies in Mycology*, 58, 157e183, (2007).

[37] J.H. Birkinshaw, A. Gowlland. *Biochemical Journal*, 84, 342-347, (1962).

[38] S.S. Shankar, A. Rai, B. Ankamwar, A. Singh, A. Ahmad, M. Sastry, *Nature materials* 3, 482–488, (2004).

[39] H. Bar, D.K. Bhui, G.P. Sahoo, P. Sarkar, S.P. De, A. Misra. *Colloids and surfaces A: Physicochemical and engineering aspects*, 339(1), 134-139, (2009).

[40] A. Baghizadeh, S. Ranjbar, V. K. Gupta, M. Asif, S. Pourseyedi, M. J. Karimi, R. Mohammadinejad. Journal of Molecular Liquids, 207, 159-163, (2015).

[41] D. Cruz, P.L. Fale, A. Mourato, P.D. Vaz, M.L. Serralheiro, A.R. Lino. *Colloid. Surface. B* 81 67–73, (2010).

[42] R. Kumar, S.M. Roopan, A. Prabhakarn, V.G. Khanna and S. Chakroborty. Spectrochimica Acta Part A: Molecular and Biomolecular Spectroscopy, 90, 173-176.

Chicago, (2012).

[43] G. Sathiyanarayanan, G.S. Kiran, J. Selvin. *Colloid. Surface. B* 102 13–20, (2013).

[44] T.Y. Suman, S.R. Radhika Rajasree, A. Kanchana, S.B. Elizabeth. *Colloid. Surface. B* 106 74–8, (2013).

[45] S. Mandal, S. Phadtare, M. Sastry. *Current Applied Physics*, 5, 118–27, (2005).

[46] A. Baghizadeh, S. Ranjbar, V.K. Gupta, M. Asif, S. Pourseyedi, M.J. Karimi, R. Mohammadinejad. *Journal of Molecular Liquids*, 207, 159-163, (2015)

[47] S.M. Roopan, G. Madhumitha, A.A. Rahuman, C. Kamaraj, A. Bharathi, T.V. Surendra. *Industrial Crops and Products*, 43, 631-635, (2013).

[48] P.S. Pimprikar. *Colloids and Surfaces B: Biointerfaces*, 7(4.1), 309-316, (2009).

[49] K. Kathiresan, *Colloids and surfaces B: Biointerfaces* 71(1), 133-137, (2009).

[50] T. Park. Nano letters, 7(3), 766-772, (2007).

[51] C. Bhainsa, C. Kuber, S.F. D'souza, *Colloids and surfaces B: Biointerfaces* 47(2), 160-164, (2006).

[52] H. Korbekandi, I. Siavash, A. Sajjad. *Critical Reviews in Biotechnology* 29 (4) 279-306, (2009).